IJST, Transactions of Mechanical Engineering, Vol. 38, No. M1, pp 135-141
Printed in The Islamic Republic of Iran, 2014

"Research Note"

DYNAMIC MODELING AND TRACKING CONTROL OF A SWIMMING MICROROBOT PROPELLED BY TWO PROKARYOTIC FLAGELLA*

H. NOURMOHAMMADI AND M. BAHRAMI**

[1]Dept. of Mechanical Engineering, Amirkabir University of Technology (Tehran Polytechnic), AUT, I. R. of Iran
Email: mbahrami@aut.ac.ir

Abstract– Swimming microrobots are miniature machines which can be designed and fabricated using microelectromechanical systems (MEMS) technology. They can play a key role in many biomedical applications, such as controlled drug delivery, microsurgery, and diseases monitoring. Many researches have been carried out on micro swimming methodologies. Also, different propulsion mechanisms have been introduced for 1-DOF microswimmers. The objective of this work is to study a flagellar microswimmer with controlled maneuvers. The propulsion mechanism used in our design contains two prokaryotic flagella, rotating into the fluid media, leading to microrobot movement. In this study, we have tried to focus on dynamic modeling of the motion proposed for the swimming microrobot. Then, an appropriate control law was developed in order to control the microrobot maneuvers. The resistive-force theory was used in order to determine the hydrodynamic force created by the rotary motion of each flagellum into the fluid media. Feedback linearization method was used to control the motion of microrobot for tracking performance. The results obtained revealed that microrobot can be controlled in such a way that the desired maneuver can be performed by applying the designed controller.

Keywords– Swimming microrobot, dynamic modeling, tracking control, prokaryotic flagella

1. INTRODUCTION

Swimming microrobot have the potential of being implanted inside human bodies and accomplishing many complex tasks, such as controlled drug delivery, monitoring of syndromes, and minimally invasive surgery [1, 2]. Such crucial applications reveal the importance of developing a maneuverable microswimmer with controlled motions. The substantial contrast between swimming at micro and macro scales arises from the hydrodynamics law corresponding regimes of fluid flows. Due to the miniature size and low velocity of swimming microrobots, their motion occurs in very low Reynolds number ($Re \ll 1$) fluid flow. In this case, the viscous forces may have dominant effects and therefore, the inertial forces can be ignored.

The most important part of the swimming microrobots is their propulsion mechanism. Three biological propulsion mechanisms are introduced to be used in swimming microrobots, inspired by swimming microorganisms in nature. These methodologies are prokaryotic flagellar motion, eukaryotic flagellar motion, and ciliary motion [3].

There is large amount of research concerning propulsion mechanisms in swimming microrobots. Behkam and Sitti developed two methodologies for swimming in very low Re fluid flows based on prokaryotic and eukaryotic flagellar motions [4, 5]. Kosa et al. presented a new propulsion mechanism for swimming at microscale based on traveling wave in an elastic tail [6]. Li et al. advanced the swimming

*Received by the editors April 21, 2013; Accepted November 2, 2013.
**Corresponding author

performance of prokaryotic microrobots by composing a prokaryotic helical head and an elastic tail [7]. Singleton et al. increased the thrust of swimming microrobot using multiple parallel flagella in the propulsion system, [8]. Ghanbari and Bahrami presented a novel propulsion methodology based on ciliary motion which is inspired by the protozoan paramecium [1]. There are other works concentrated on the control of swimming microrobots in the literature. Mahoney et al. designed a velocity control for a magnetically actuated flagellar microswimmer [9]. Marino et al advanced robust H_∞ technique to control the motion of an electromagnetic microswimmer in the presence of some parameters uncertainty [10].

Dynamic model of one degree-of-freedom flagellar swimming microrobot was studied in the previous works. However, here we have tried to advance the dynamic model of two degrees-of-freedom maneuverable swimming microrobot and then, design an appropriate controller to control the microrobot's maneuvers.

2. DYNAMIC MODELING

Inspired by the motion of microorganisms, we propose a flagellar swimming microrobot which is propelled by two prokaryotic flagella and has the ability of doing 2-D maneuvering. The schematic view of the proposed microrobot and the prokaryotic flagella are shown in Fig. 1.

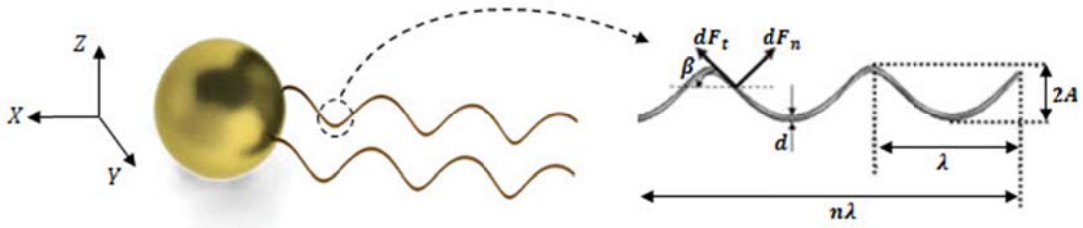

Fig. 1. Schematic view of a swimming microrobot propelled by two prokaryotic flagella

According to the viscosity of the fluid and rotational frequency of flagellum, a hydrodynamic force acts on the flagellum when the prokaryotic flagellum rotates in the fluid media. This force results in propulsion in the swimming microrobot. The geometrical parameters of the helical flagellum and the normal and tangential components of the hydrodynamic force, exerted on each flagellum, are specified in the Fig. 1.

We have applied resistive-force theory (RFT) to derive the normal and tangential components of the viscous hydrodynamic force [11]. Considering element *ds* along the helical flagellum and using RFT, the corresponding normal and tangential components (dF_n, dF_t) of the viscous force are calculated. The equations driven are shown below:

$$dF_i = -C_i V_i ds \qquad i = n, t \tag{1}$$

The resistive coefficients for a helical flagellum (C_n and C_t) are obtained as follows [12]:

$$C_n = \frac{4\pi\mu}{\ln\left(\frac{0.18\lambda}{d}\right)+\frac{1}{2}}, \quad C_t = \frac{2\pi\mu}{\ln\left(\frac{0.18\lambda}{d}\right)} \tag{2}$$

Composing the normal and tangential components of F_n and F_t, the resultant force and torque along and about of the *X*-direction for each flagellum is obtained by:

$$\begin{aligned} dF_X &= dF_t \cos\beta - dF_n \sin\beta \\ dM_X &= -A\,(dF_t \sin\beta + dF_n \cos\beta) \end{aligned} \tag{3}$$

The normal and tangential velocities of the element *ds* can be obtained from Eq. (4):

$$\begin{aligned} V_n &= -\dot{X}\sin\beta + A(\omega-\dot{\theta})\cos\beta \\ V_t &= \dot{X}\cos\beta + A(\omega-\dot{\theta})\sin\beta \end{aligned} \tag{4}$$

Where, ω and $\dot{\theta}$ are the input angular velocity of system and resistive angular velocity constructed by M_X respectively. Furthermore, there is an additional viscous torque constituted through hydrodynamic reaction between the helical flagella and surrounding the fluid flow. The *X*-component of this torque is obtained by Eq. (5) [12]:

$$M_S = n\lambda\pi\mu d^2\dot{\theta}\cos\beta \tag{5}$$

The body of microrobot is considered as a sphere with the radius of *a*. Two prokaryotic flagella are symmetrically located on the diameter of sphere along the *Y*-direction. Disregarding the inertial terms, the governing equations, corresponded to microrobot's motion, would be set up through force and momentum equilibrium equations as follows:

$$\begin{aligned} \sum F_{\text{X,helix}} + F_{\text{X,body}} &= 0 \\ \sum M_{\text{Z,helix}} + M_{\text{Z,body}} &= 0 \end{aligned} \tag{6}$$

Where, $F_{X,body}$ and $M_{X,body}$ characterize the drag force and torque, respectively. Considering Stokes flow, the drag force and torque for a sphere with the radius of a are calculated by:

$$\begin{aligned} F_{\text{X,body}} &= 6\pi\mu a\dot{X} \\ M_{\text{Z,body}} &= 8\pi\mu a^3\dot{\varphi} \end{aligned} \tag{7}$$

In which $\dot{\varphi}$ is the angular velocity of microrobot body about *Z*-axis. Substituting Eqs. (1) and (4) in the Eq. (3) and integrating for $X \in [0 \;\; n\lambda]$ leads to:

$$\begin{aligned} F_{i,X} &= An\lambda(C_n - C_t)(\omega_i - \dot{\theta})\sin\beta - n\lambda(C_n\sin^2\beta\sec\beta + C_t\cos\beta)\dot{X}, \quad i = 1,2 \\ M_{i,X} &= A^2 n\lambda(C_n\cos\beta + C_t\sin^2\beta\sec\beta)(\omega_i - \dot{\theta}) - (An\lambda(C_n - C_t)\sin\beta)\dot{X}, \quad i = 1,2 \end{aligned} \tag{8}$$

Moreover, the magnitude of $\dot{\theta}$ is determined according to momentum equation about *X*-axis:

$$M_{1,X} + M_{2,X} + 2M_S = 0 \tag{9}$$

Substituting the Eqs. (5), (7) and (8) in the Eqs. (6) and (9), the forward velocity of microswimmer and its angular velocity about *Z*-axis would be obtained as:

$$\begin{aligned} \dot{X} &= \frac{p_1}{4p_2^2 - 2p_3p_4}(\omega_1 + \omega_2) \\ \dot{\varphi} &= \frac{p_2}{p_5}(\omega_1 - \omega_2) \end{aligned} \tag{10}$$

Parameters p_1 to p_5 are defined in the terms of geometrical parameters of flagella and hydrodynamic properties of fluid media, in the set of relations in Eq. (11).

$$\begin{aligned} p_1 &= A\,n^2\lambda^2\pi\mu d^2(C_n - C_t)\sin 2\beta \\ p_2 &= A\,n\lambda(C_n - C_t)\sin\beta \\ p_3 &= A^2 n\lambda(C_n\cos\beta + C_t\sin^2\beta\sec\beta) - n\lambda\pi\mu d^2\cos\beta \\ p_4 &= 2n\lambda(C_n\sin^2\beta\sec\beta + C_t\cos\beta) + 6\pi\mu a \\ p_5 &= 8\pi\mu a^3/b \end{aligned} \tag{11}$$

Equation (10) shows that when ω_1 and ω_2 are equal to each other, there is no rotation about *Z*-axis. Therefore, microrobot can move along a straight line without any maneuvering. However, when each flagellum rotates with different frequencies, the microrobot can rotate continuously and move in two-dimensional path.

3. TRACKING CONTROL

Taking into account biomedical applications of the swimming microrobots, the necessity of control in this work would be appreciated. In the current section, attention is focused on the tracking performance of microrobot, i.e. making it maneuver in the desired way and move along the desired path. Feedback linearization method is utilized to guarantee this purpose. However, there are some other methods to design tracking controller (e.g. sliding mode control) [13].

It should be noticed that Eq. (10) is defined in body coordinates which continuously rotate when the microrobot moves only along a non-straight line. Defining (*x*-*y*-*z*) as reference coordinates (see Fig. 2), the forward velocity of $\dot{X}$ divides in two components:

$$\begin{cases} \dot{x} = \dot{X}\cos(\varphi) \\ \dot{y} = \dot{X}\cos(\varphi) \end{cases} \tag{12}$$

And the rotation angle of φ changes with dynamic shown in Eq. (10). Considering function of $y_d = f(x_d)$ as a general form of desired path, the rotation angle, corresponded to this curve can be determined through following relation.

$$\varphi = \cos^{-1}\left(\frac{\dot{x}}{\dot{X}}\right) = \cos^{-1}\left(\frac{\dot{x}}{\sqrt{\dot{x}^2 + \dot{y}^2}}\right) = \cos^{-1}\left(\frac{dx}{\sqrt{dx^2 + dy^2}}\right) \tag{13}$$

Using Eq. (13), the desired value of φ_d is specified. The control strategy is that the system inputs (i.e. the angular speed of each flagellum) must be controlled in a way that the rotation angle φ tracks the desired value of φ_d. Using feedback linearization method, the control law for tracking performance of the proposed microswimmer can be defined by following equation [14]:

$$\omega_1 - \omega_2 = \frac{p_5}{p_2}(\dot{\varphi}_d - k\,\tilde{\varphi}) \tag{14}$$

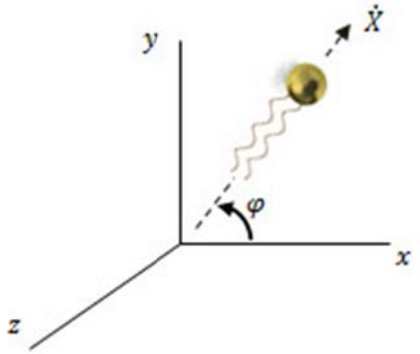

Fig. 2. Reference coordinates (*x*-*y*-*z*) and rotation angle (φ)

Where, *k* is a positive constant and $\tilde{\varphi}$ is the tracking error $(\tilde{\varphi} = \varphi - \varphi_d)$. Note that the difference between angular velocity of each flagellum $(\omega_1 \text{ and } \omega_2)$ is the be-all and end-all of making rotation and maneuver in the microswimmer. The control law of the Eq. (14) can alter this difference in such a way that system

behaves in a desired manner. In Eq. (14), ω_2 can be selected arbitrary and therefore ω_1 is determined. The greater value of ω_2 causes the faster tracking performance. In the prokaryotic microorganisms, flagella rotate at speed about *100 Hz* [15]. Substituting the control law of Eq. (14) in the dynamic model of Eq. (10) leads to:

$$\dot{\tilde{\varphi}} + k\,\tilde{\varphi} = 0 \tag{15}$$

The Eq. (15) is so-called tracking error dynamic. The stability of error dynamic is guaranteed bearing in mind the positive constant of k. On the other hand, the tracking error is converged to zero and the perfect tracking is exponentially satisfied.

4. RESULTS AND DISCUSSION

In this section, we focus on the simulated results of the flagellar swimming microrobot which was dynamically modeled and controlled. It has been assumed in the simulation that both flagella are made of similar steel filament having equal geometry. Furthermore, the biofluid media, in which the microrobot swims, has the same hydrodynamics features as water. The body of microrobot is considered as a sphere with a radius of *1.5 μm*. Table 1 expresses the geometrical properties of each flagellum.

Table 1. Geometrical properties of the prokaryotic flagella used in the microrobot

Parameters	Dimensions (μm)
Wavelength, λ	0.7
Total length, $n\,\lambda$	3.5
Filament diameter, d	0.02
Amplitude, A	0.25
Offset distance, b	1.0

To investigate the controller performance, a close-loop test is designed. In this test, the desired path is considered as an arbitrary curve of Eq. (16):

$$y_d = 10^7 x_d^2 \tag{16}$$

Note that the coefficient of 10^7 is a normalizing factor to amplify the magnitude of y_d. The simulation results of the close-loop test are illustrated in Figs. 3 and 4.

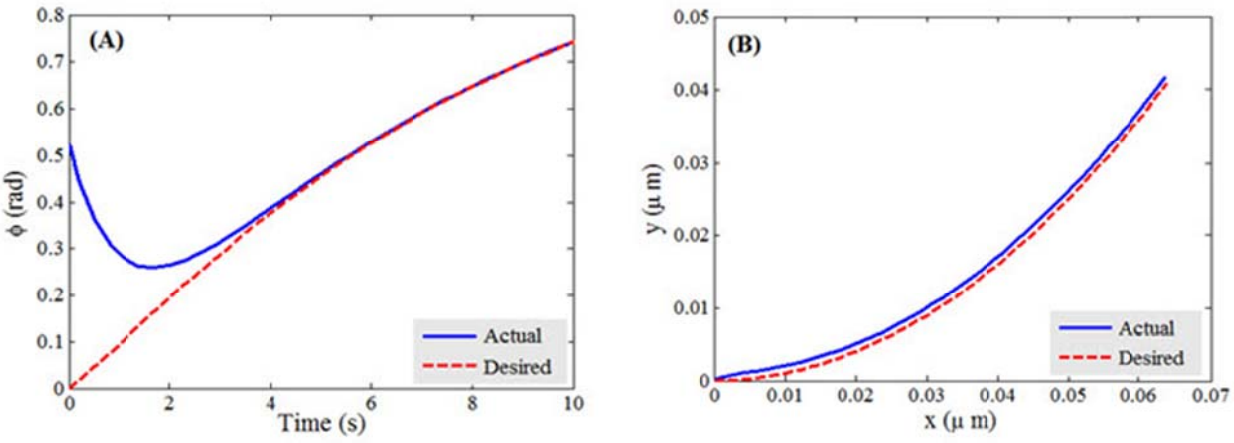

Fig. 3. Simulation result of the close-loop system by applying feedback linearization method. A) Tracking of the rotation angle φ. B) Path tracking performance of swimming microrobot

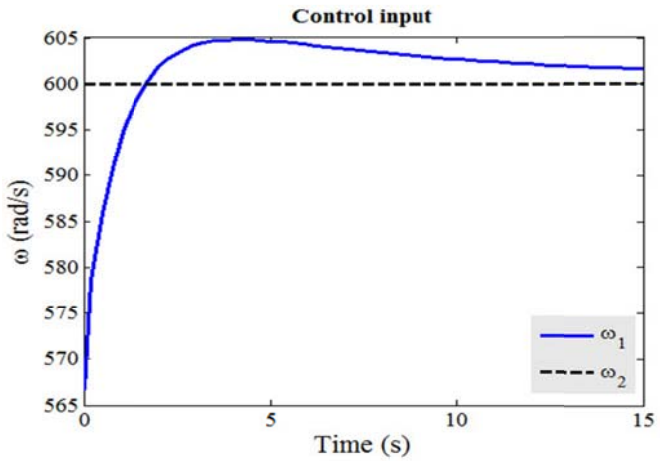

Fig. 4. Required values of angular speed of each flagellum in the close-loop model (control input)

The initial value of φ has been considered as $\pi/6$ and the microrobot has been initially located at the origin of reference coordinates. The rotation angle variation rate ($\dot{\varphi}$) will be reduced over the time. After four seconds, it will be changed with fewer gradients. In this situation, the magnitude of ω_1 would reach ω_2. In the simulation, the magnitude of ω_2 has been chosen as 600 *rad/s* and then, the angular speed of first flagellum has been determined through the control law of Eq. (14). At the beginning, the rotational angles tend to be changed with higher gradient. In this vicinity, a larger control effort is required. However, by the tracking error reduction, a gradual decrease may occur in the control effort. Results obtained from simulation show that, tracking error between φ and φ_d converges to zero. As a result of this convergence, microrobot follows the desired path.

5. CONCLUSION

Biomedical applications of swimming microrobots make them attractive, particularly in medical and biomechanics fields. These microdevices have the potential of entering in the human body and accomplishing many complex operations. These show the necessity of developing a maneuverable and controllable medical microrobot. The main part of swimming microrobots is the propulsion mechanism. Based on flagellar motion, we have applied two prokaryotic flagella for propulsion. In our design, the viscous forces had a significant role compared to inertial forces. Resistive-force theory was utilized to derive the propulsion force created by each flagellum. It has been shown that when each flagellum spins with different frequency, microrobot rotates about *z*-axis and moves along a circular path in the *x*-*y* plane. After dynamic modeling of the entire system of the proposed microrobot, tracking control was considered. Making microrobot follow the desired path is the objective of the control. To acquire this purpose, feedback linearization method was utilized. Results obtained from simulation show that applying the designed controller results in perfect tracking guaranteed with considerable accuracy. However, advancing swimming microrobots to have the ability of doing three-dimensional motion was the main challenge, and can be studied in the future works.

REFERENCES

1. Ghanbari, A. & Bahrami, M. (2011). A novel swimming microrobot based on artificial cilia for biomedical application. *J Intelligent and Robotic Systems*, Vol. 63, pp. 399-416.
2. Nelson, B. J., Kaliakatsos, I. K. & Abbott, J. J. (2010). Microrobots for minimally invasive medicine. *Annu Rev Biomed Eng*, Vol. 12, pp. 55-85.

3. Abbott, J. J., Peyer, K. E., Lagomarsino, M. C. & et al. (2009). How should microrobots swim? *J Robotics Research*, Vol. 28, pp. 1434-1447.
4. Behkam, B. & Sitti, M. (2006). Design methodology for biomimetic propulsion of miniature swimming robot. *Trans ASME J Dynamic Systems, Measurement and Control*, Vol. 128, pp. 36-43.
5. Behkam, B. & Sitti, M. (2004). E-coli inspired propulsion for swimming microrobots. *Proceeding of ASME International Mechanical Engineering Conference and Exposition*, pp.1037-1041.
6. Kosa, G., Shoham, M. & Zaaroor, M. (2007). Propulsion method for swimming microrobots. *IEEE Transaction on Robotics*, Vol. 23, pp. 137-150.
7. Li, H., Tan, J. & Zhang, M. (2009). Dynamics modeling and analysis of a swimming microrobot for controlled drug delivery. *IEEE Transactions on Automation Science and Engineering*, Vol. 6, pp. 220-227.
8. Singleton, J. & et al. (2011). Micro–scale propulsion using multiple flexible artiticial Flagella. *International conference on Intelligent Robots and Systems, San Francisco*, pp.1687-1692.
9. Mahoney, A., Sarrazin, J. C., Bamberg, E. & Abbott, J. J. (2011). Velocity control with gravity compensation for magnetic helical microswimmers. *J Advanced Robotics*, Vol. 25, pp. 1007–1028.
10. Marino, H., Bergeles, C. & Nelson, B. J. (2012). Robust H∞ control for electromagnetic steering of microrobots. *IEEE International Conference on Robotic and Automation (ICRA)*.
11. Hancock, G. (1953). The self-propulsion of microscopic organisms through liquids. *Proc. R Soc. London, Ser. A*, Vol. 217, pp.96-121.
12. Lighthill, J. (1976). Flagellar hydrodynamics. *SIAM Review*, Vol. 18, pp.161-230.
13. Guclu, R. & Yagiz, N. (2004). Comparison of different control strategies on a vehicle using sliding mode control. *Iranian Journal of Science & Technology, Transactions of Mechanical Engineering*, Vol. 28, pp. 413-422.
14. Slotine, E. (1991). *Applied nonlinear control*. New Jersey: Prentice Hall.
15. Leifson, E. (1960). *Atlas of bacterial flagellation*. New York, Academic press.